

## Living Tokay Geckos Display Adhesion Times Following Weibull Statistics

Nicola M. Pugno and Emiliano Lepore

Department of Structural Engineering and Geotechnics, Politecnico di Torino, Torino, Italy

*In this paper we demonstrate that living tokay geckos (*Gekko gekko*) display adhesion times following Weibull Statistics. We have considered two different geckos, male or female, adhering on different surfaces, glass, or Poly(methyl methacrylate) (PMMA) with different roughness. We have performed detailed surface topography characterizations by means of a three-dimensional optical profilometer. The analysis suggests the existence of a “weakest link” in the gecko adhesion and is able to quantify its degree of brittleness in different systems.*

**Keywords:** Adhesion time; Living gecko; Optical profilometer; Surface roughness; Three-dimensional characterization; Weibull statistics

### 1. INTRODUCTION

In the world, there are more than 1050 species of geckos divided in 50 families. The tokay gecko (*Gekko gekko*) is the second largest gecko species: an individual can weigh up to 150–200 grams. The tokay gecko’s climbing ability has attracted human attention for more than two millennia. The gecko’s ability to “run up and down a tree in anyway, even with the head downwards” has been observed since the time of Aristotle [1], who mentioned these curious creatures in his manuscript, *Historia Animalium*, written four centuries before Christ.

Until the mid-twentieth century, scientific observations have not permitted a good understanding of the capacity of the gecko to stay stuck motionless or running on vertical or inverted surfaces

Received 4 April 2008; in final form 15 September 2008.

Address correspondence to Nicola M. Pugno, Department of Structural Engineering and Geotechnics, Politecnico di Torino, Corso Duca degli Abruzzi 24, 10129 Torino, Italy. E-mail: nicola.pugno@polito.it

[2–5]. Only after the electron microscopy’s development, in the 1950s, were researchers able to note the hierarchical, from the nano- to the macro-scale, morphology of the gecko’s feet [6–10]. A typical tokay gecko foot consists of hierarchical structures (Figure 1) starting with macroscopic lamellae (soft ridges,  $\sim 1$  mm in length), from which branch off setae (30–130  $\mu\text{m}$  in length and 5–10  $\mu\text{m}$  in diameter). Every seta terminates with 100–1000 substructures called spatulae (0.1–0.2  $\mu\text{m}$  wide and 15–20 nm thick), responsible for gecko adhesion. More recently, numerous studies (see [11–22] and related references) bring out the factors that allow the gecko to adhere and detach from surfaces. Very recently, van der Waals attraction [21] and capillarity [22] have been recognized as the key mechanisms in the gecko adhesion.

Like geckos, many other creatures such as beetles, flies, and spiders possess remarkable ability to move on vertical surfaces and ceilings (e.g., see [23,24] and related references). Their adhesive ability arises from the micro/nanostructures of which their attachment pads are

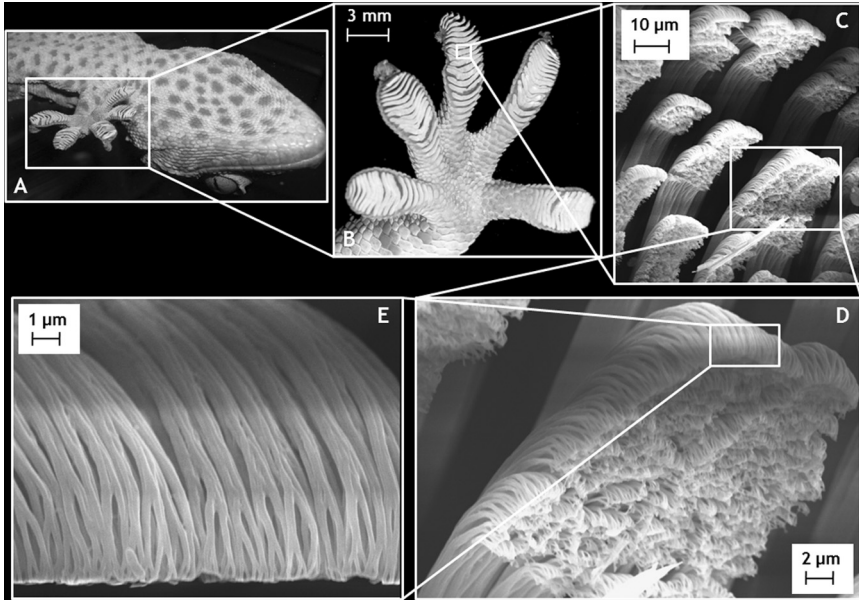


**FIGURE 1** Hierarchical gecko adhesion apparatus. (A) Ventral view of the tokay gecko (*Gekko gecko*). (B) Gecko’s foot. Scanning electron microscope (SEM) micrographs of (C) the setae, (D) at higher magnification, (E) terminating in hundreds of spatulae.

composed. It is noteworthy that as the mass of the creature increases, the size of the terminal attachment elements decreases and their density increases [15], in order to enhance the adhesion strength. Thus, more than insects and spiders, geckos exhibit the most versatile and effective dry adhesion known in nature, as imposed by their larger mass. Mimicking gecko adhesion could lead to a revolution in material science [25–27] and Spiderman suits are also envisioned [27].

In this paper we report new observations on the adhesion times of living tokay geckos. We have considered two different geckos, male or female, adhering on different surfaces, glass or Poly(methyl methacrylate) (PMMA) with different roughness. Previously, all these surfaces were analysed with a three-dimensional optical profilometer. The data have been treated using Weibull statistics, showing a relevant statistical correlation.

Although the measurement of failure time is an interesting parameter, it cannot be directly correlated with the force and energy values of prior studies. Moreover, since our data were from live geckos, the role of animal behavior in failure time cannot be *a priori* excluded and the adhesion times have to be considered as indicative of the entire biosystem, *i.e.*, not only of the animal's adhesion ability but, for example, also of muscular fatigue (it is well-known that geckos must produce shear forces to maintain adhesive forces [19]: given the long attachment times, it is reasonable that the geckos became fatigued, limiting their clinging ability). Nevertheless, the extraordinary adhesion ability that we have observed after the moult suggests to us that the adhesion times that we have measured are mainly linked to the adhesion ability and scarcely influenced by other factors, such as muscular fatigue.

## 2. SURFACE CHARACTERIZATION

The characterization of PMMA and glass surfaces was performed with a three-dimensional optical profilometer, Talysurf CLI 1000, equipped with the CLA Confocal Gauge 300 HE (300  $\mu\text{m}$  range and 10 nm vertical resolution), both from Taylor Hobson, Leicester, UK. The parameters tuned during the analysis are the measurement speed (50  $\mu\text{m}/\text{s}$ ), the sampling rate (100 Hz), the measured area (0.1  $\times$  0.1 mm), the resolution in the “xy” plane (0.5  $\mu\text{m}$ ), leading to a final resolution of 201 points/profile. All parameters were referred to a 25  $\mu\text{m}$  cut-off.

The roughness parameters considered in the analysis were Sa, Sq, Sp, Sv, Sz, Ssk, and Sdr. Sa represents the surface's arithmetical average roughness; Sq is the mean square roughness (the mean

square deviation of the profile from the middle line);  $S_p$  and  $S_v$  are, respectively, the height of the highest peak and the depth of the deepest valley (absolute value);  $S_z$  is the average distance between the five highest peaks and the five deepest valleys detected in the analyzed area. The last two parameters ( $S_{sk}$  and  $S_{dr}$ ) are expressive of the surface's skewness and three-dimensionality.  $S_{sk}$  indicates the surface skewness: if  $S_{sk}$  is 0 the surface is equally distributed on the middle line; when lower than 0 it describes a surface with plateau and several deep thin valleys, whereas when higher than 0 a plateau and several peaks.  $S_{dr}$  is the ratio between the effective and projected areas, minus one; thus it, describes the surface's three-dimensionality.

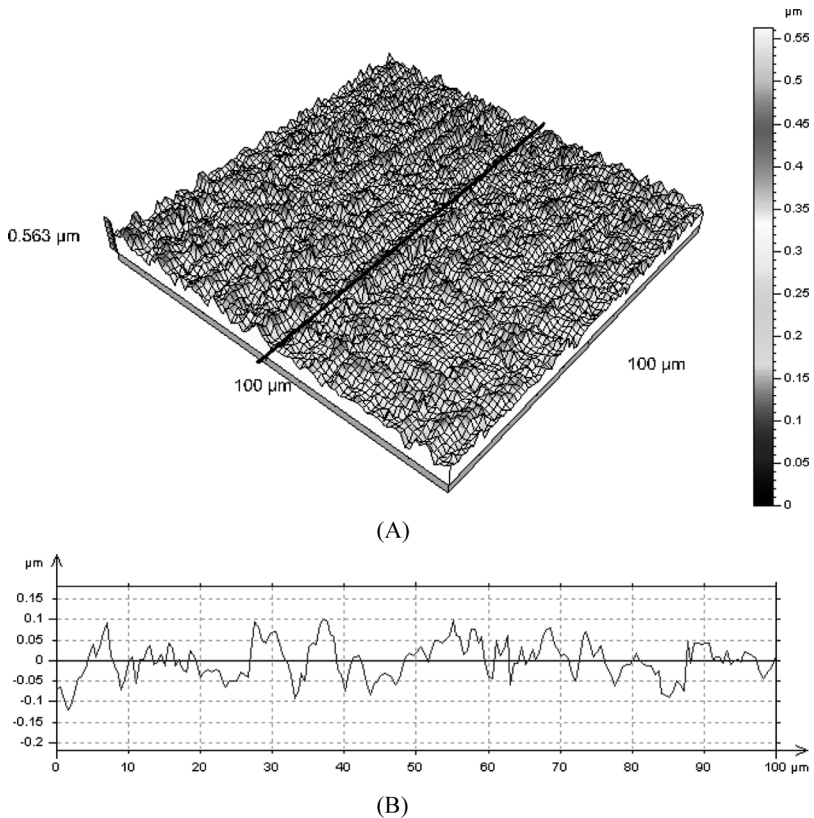


**FIGURE 2** PMMA virgin surface. (A) Three-dimensional topography. (B) Two-dimensional profile (extracted at  $50\mu\text{m}$  from the edge of the square measured area).

Virgin PMMA and glass surfaces nearly present homogeneous roughness without significant anomalous alterations, apart from small isolated bubbles on the surface of the glass derived from melting during the fabrication process. Figures 2 and 3 show the virgin PMMA and glass surface (A) three-dimensional topographies and (B) two-dimensional profiles. PMMA surfaces with different roughness, namely PMMA2400 or PMMA800, have been also considered. PMMA2400/800 surfaces are obtained by a manual process that consists in doing clockwise circular movement for 2 minutes on the material sample using sand-paper 2400/800. Figures 4 and 5 show the PMMA2400/800's surface (A) topographies and (B) profiles. We note that the roughness parameters allow us to appreciate the differences between virgin PMMA and glass surfaces and more importantly become nearly one order of magnitude

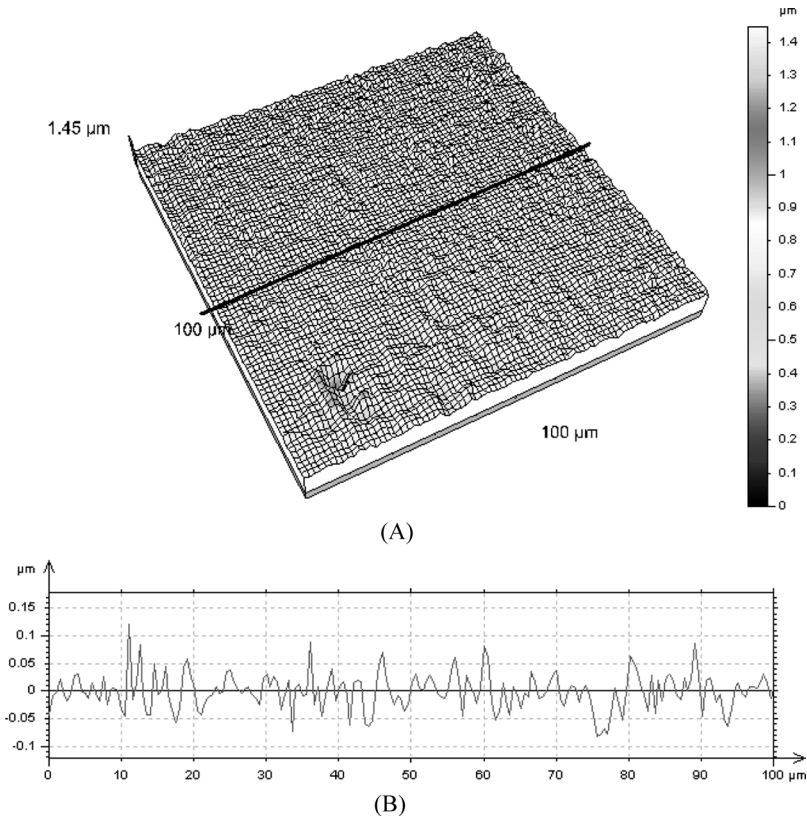


**FIGURE 3** Glass surface. (A) Three-dimensional topography. (B) Two-dimensional profile (extracted at 50  $\mu\text{m}$  from the edge of the square measured area).

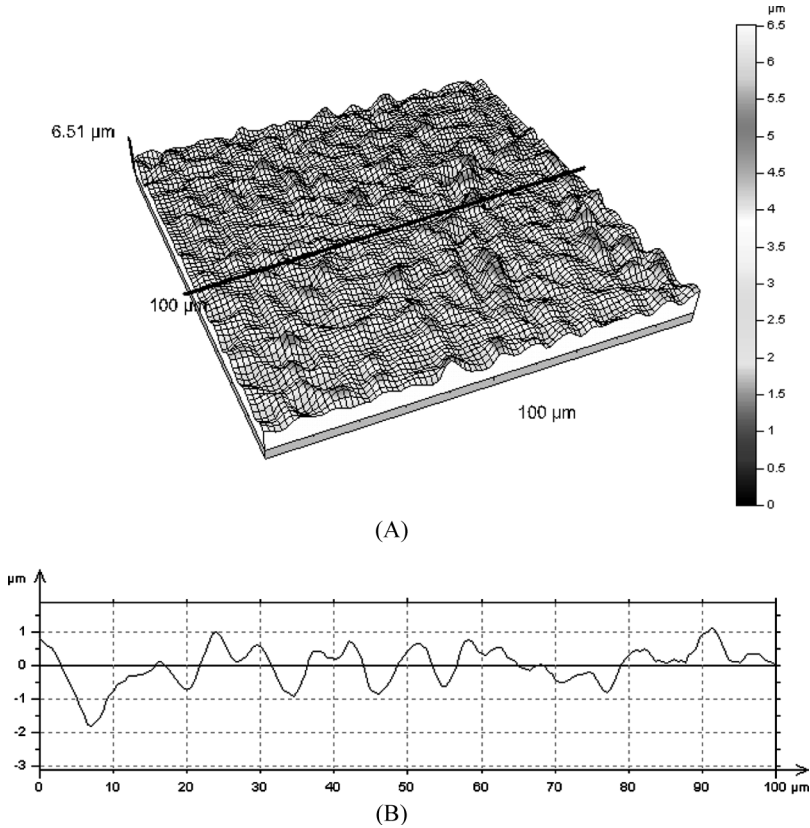


**FIGURE 4** PMMA2400 surface. (A) Three-dimensional topography. (B) Two-dimensional profile (extracted at  $50\ \mu\text{m}$  from the edge of the square measured area).

greater for machined PMMA surfaces (with the exception of the skewness that however changes its sign). Table 1 summarizes average roughness parameters of all the characterized surfaces.

### 3. WEIBULL STATISTICS

We analysed the gecko's adhesion times using the well-known Weibull statistics. It is usually applied to describe the strength and fatigue life of solids, since it is based on the weakest link concept. Thus, we treat the gecko detachment as an interfacial failure. The discovered significant statistical correlation suggests the existence of a weakest link

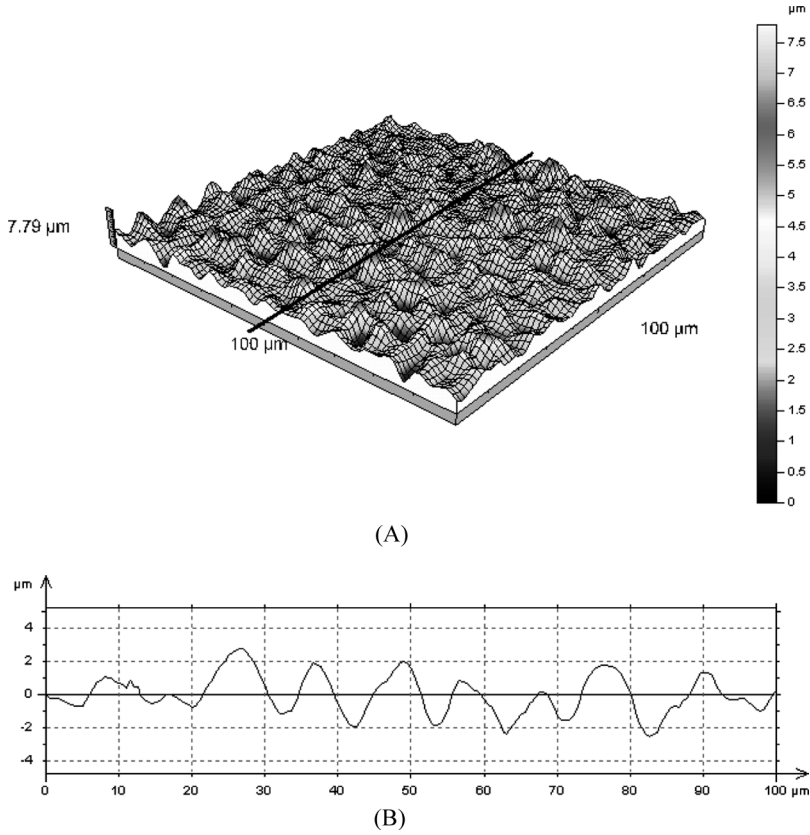


**FIGURE 5** PMMA800 surface. (A) Three-dimensional topography. (B) Two-dimensional profile (extracted at 50  $\mu\text{m}$  from the edge of the square measured area).

**TABLE 1** Roughness Parameters of the Characterized Surfaces

	Glass	PMMA	PMMA2400	PMMA800
Sa ( $\mu\text{m}$ )	$0.031 \pm 0.0019$	$0.033 \pm 0.0034$	$0.481 \pm 0.0216$	$0.731 \pm 0.0365$
Sq ( $\mu\text{m}$ )	$0.041 \pm 0.0034$	$0.042 \pm 0.0038$	$0.618 \pm 0.0180$	$0.934 \pm 0.0382$
Sp ( $\mu\text{m}$ )	$0.366 \pm 0.1649$	$0.252 \pm 0.0562$	$2.993 \pm 0.1845$	$4.620 \pm 0.8550$
Sv ( $\mu\text{m}$ )	$0.434 \pm 0.2191$	$0.277 \pm 0.1055$	$2.837 \pm 0.5105$	$3.753 \pm 0.5445$
Sz ( $\mu\text{m}$ )	$0.609 \pm 0.2791$	$0.432 \pm 0.1082$	$4.847 \pm 0.2223$	$6.977 \pm 0.2294$
Ssk	$-0.381 \pm 0.4630$	$-0.122 \pm 0.1103$	$0.171 \pm 0.1217$	$0.192 \pm 0.1511$
Sdr (%)	$0.574 \pm 0.0724$	$0.490 \pm 0.0214$	$15.100 \pm 1.6093$	$28.367 \pm 2.2546$

in the animal's adhesion, rigorously quantified by the Weibull shape and scale parameters by data fitting.

Accordingly, the distribution ( $F$ ) describing the cumulative probability for gecko detachment is expected to be:

$$F(t; m; t_0) = 1 - e^{-\left(\frac{t}{t_0}\right)^m}, \quad (1)$$

where  $t$  is the measured adhesion time,  $m$  is the shape parameter (governing the standard deviation), or Weibull modulus, and  $t_0$  is the scale parameter (governing the mean value) of the distribution of failure.

The cumulative probability  $F_i(t_i)$  can be obtained experimentally as:

$$F_i(t_i) = \frac{i - 1/2}{N}, \quad (2)$$

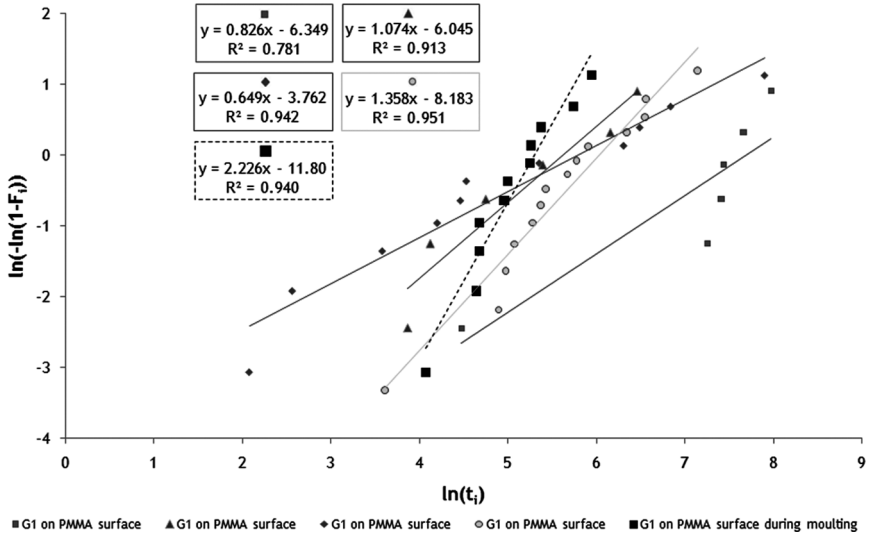
where  $N$  is the total number of measured adhesion times  $t_i$ , and  $t_1, \dots, t_N$  are ranked in ascending order.

We considered a female gecko (G1) adhering on inverted PMMA or glass surfaces under only its weight ( $\sim 46$  g). The animal was placed in its natural position on the horizontal bottom of a box ( $50 \times 50 \times 50$  cm<sup>3</sup>) composed of the characterized surfaces. Then, slowly, we rotated the box, so that the gecko reached its downwards position; at that time we started to measure the gecko time of adhesion. We excluded any trial in which the gecko walked on the inverted surface; the time measurement was stopped when gecko broke loose from the inverted surface and jumped on the bottom of the box. A similar analysis was carried out with a male gecko (G2, weight of  $\sim 72$  g), but in this case the time was stopped at the first detachment movement of the gecko's feet. The different measurement strategies do not significantly affect the statistics of the results, confirming their robustness.

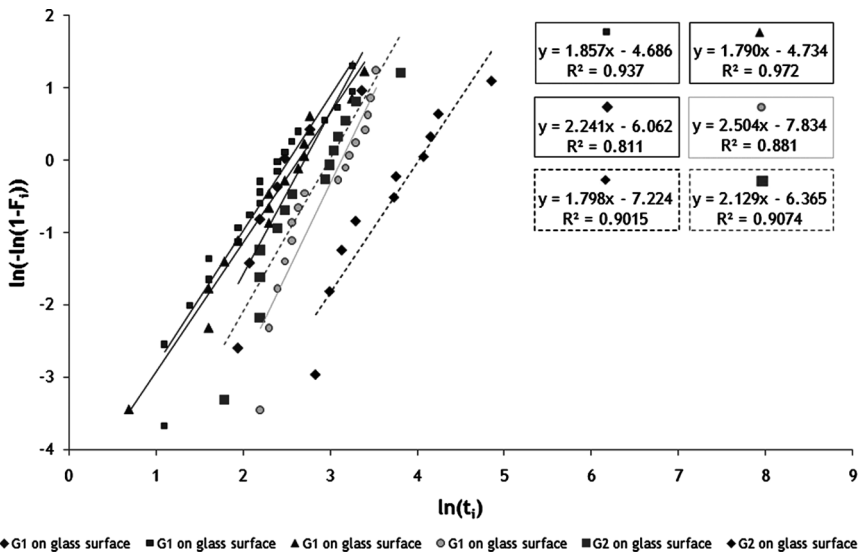
All experiments were performed at ambient temperature ( $\sim 23^\circ\text{C}$ ) and humidity ( $\sim 75\%$ ). Each set of measurements was performed during different days. The time between one measurement and the following, pertaining to the same set, is only the time needed to rotate the box ( $\approx 14$  s), in order to place the gecko again in its downwards position.

Figure 6 presents the Weibull statistics applied to the five measurements of the adhesion of G1 on a virgin PMMA surface; only one set is taken during the moult (X-dots). Similarly, Figure 7 shows the Weibull interpretation for four sets of G1 and two of G2 (dashed lines) on the glass surface. Table 2 summarizes the values of the Weibull modulus,





**FIGURE 6** Weibull statistics on G1 applied to the four data sets and in case of moul (X-dots), on virgin PMMA.



**FIGURE 7** Weibull statistics applied to the four data sets of G1 and the two data sets of G2 (dashed lines), on glass.

$m$  (shape parameter), and of the scale parameter,  $t_0$ , for each set on PMMA ( $m_{\text{PMMA}}$  and  $t_{0\text{PMMA}}$ ) or glass ( $m_{\text{Glass}}$  and  $t_{0\text{Glass}}$ ).

Considering the average values for virgin PMMA, the Weibull modulus is found to be  $m_{\text{PMMA}} \approx 1.0$  and the scale parameter is  $t_{0\text{PMMA}} \approx 800$  s (corresponding to 13 minutes and 20 s). The test during the moult shows completely different Weibull statistics, namely  $m_{\text{PMMA-M}} \approx 2.2$  and  $t_{0\text{PMMA-M}} \approx 200$  s (corresponding to 3 minutes and 20 s). For all the tests the statistical correlation  $R^2$  is found to be significant, often  $>0.9$ . Similarly, for glass the Weibull modulus is  $m_{\text{Glass}} \approx 2.0$  and the scale parameter is  $t_{0\text{Glass}} \approx 23$  s, one order of magnitude lower than for PMMA. Again, the statistical correlation  $R^2$  is found to be  $>0.8-0.9$ .

Note that larger values of  $m$  describe more deterministic processes; thus, the moult increases the deterministic nature of the adhesion and renders the PMMA comparable with the glass, see Table 3 for a direct comparison. On glass and on PMMA during the moult the ability of the gecko to keep adhering drastically decreases: the gecko realizes adhesion with several difficulties. This leads to less spread measurements and we can argue that, on glass and on virgin PMMA during the moult, the gecko's detachment is probably limited by the adhesion strength rather than by other mechanisms, *e.g.*, muscular fatigue. Moreover, the repeatability observed during different testing days confirms a scarcity of influence of external factors.

**TABLE 2** Weibull Modulus  $m$  (Shape Parameter) and the Scale Parameter  $t_0$  for Each Gecko and Set, on Virgin PMMA ( $m_{\text{PMMA}}$  and  $t_{0\text{PMMA}}$ ) and on Glass ( $m_{\text{Glass}}$  and  $t_{0\text{Glass}}$ )

	PMMA		Glass	
	Shape parameter $m_{\text{PMMA}}$	Scale parameter $t_{0\text{PMMA}}$ (s)	Shape parameter $m_{\text{Glass}}$	Scale parameter $t_{0\text{Glass}}$ (s)
Gecko G1				
1 set	0.826	2178.6	1.857	12.5
2 set	1.074	278.2	1.79	14.1
3 set	0.649	329.2	2.241	15.0
4 set	1.358	413.9	2.504	22.8
Gecko G2				
1 set	\	\	1.798	55.6
2 set	\	\	2.129	19.9
Average value	0.977	800.0	2.053	23.3

**TABLE 3** Adhesion Times on Virgin PMMA (a) During the Moulting, (b) on Glass Surface, and (c) on Virgin PMMA Not During the Moulting

(a)		(b)		(c)	
PMMA during moulting		Glass		PMMA	
Test no.	Time (s)	Test no.	Time (s)	Test no.	Time (s)
1	59	1	9	1	8
2	104	2	10	2	13
3	108	3	11	3	36
4	108	4	12	4	67
5	142	5	13	5	87
6	148	6	13	6	93
7	190	7	14	7	212
8	192	8	15	8	550
9	216	9	22	9	660
10	310	10	24	10	936
11	380	11	25	11	2703
		12	27		
		13	30		
		14	31		
		15	32		
		16	34		

We continued to observe the adhesion ability of gecko G1 during the phase following the moulting; we observed an extraordinary increase of the time of adhesion, of about 1000% for PMMA and 20000% for glass, corresponding to adhesion times of hours. This again confirms that the predominant cause of gecko detachment is its adhesion ability and that such an ability is limited by pollutant factors, efficiently removed by the moulting.

We have also tested machined PMMA2400/800 surfaces. Figure 8 presents the Weibull statistics applied to the results of one set of gecko G1 on the PMMA2400 surface and two sets of gecko G2 on both PMMA2400 and PMMA800. On PMMA2400, the Weibull modulus is basically the same for both G1 and G2 and corresponds to  $m_{\text{PMMA2400-G1}} \approx m_{\text{PMMA2400-G2}} \approx 1.2$ , with a statistical correlation  $R^2 \approx 0.95$ . For gecko G1 the scale parameter is  $t_{0-\text{PMMA2400-G1}} \approx 1618$  s (corresponding to almost 27 minutes); the scale parameter for gecko G2 is  $t_{0-\text{PMMA2400-G2}} \approx 886$  s (approximately corresponding to 15 minutes). On PMMA800, the identified Weibull modulus is  $m_{\text{PMMA800-G2}} = 1.1$  and the correlation is  $R^2 = 0.83$ . The scale parameter for gecko G2 is  $t_{0-\text{PMMA800-G2}} \approx 108$  s (corresponding to 1 minute and 48 s).

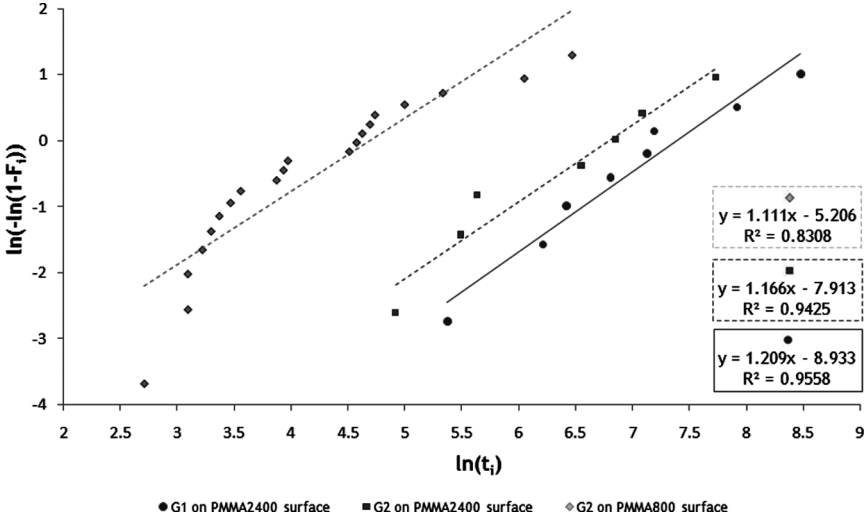


**FIGURE 8** Weibull statistics applied to the data set of G1 on PMMA2400 and to the two data sets of G2 on PMMA2400 and PMMA800.

Considering all the analyzed PMMA surfaces, both the virgin and machined ones, we have found a value of the Weibull modulus in the restricted range  $m_{PMMA} = 1-1.2$ , suggesting that this value could be a characteristic of the PMMA/gecko system. Moreover, comparing PMMA2400 and PMMA800, we note that  $t_{0-PMMA800}$  is one order of magnitude lower than  $t_{0-PMMA2400}$  or  $t_{0PMMA}$ .

**TABLE 4** Weibull Modulus  $m$  (Shape Parameter) and the Scale Parameter  $t_0$  for Each Gecko and Set, on PMMA2400 ( $m_{PMMA2400}$  and  $t_{0-PMMA2400}$ ) and on PMMA800 ( $m_{PMMA800}$  and  $t_{0-PMMA800}$ )

	PMMA2400		PMMA800	
	Shape parameter $m_{PMMA2400}$	Scale parameter $t_{0PMMA2400}$ (s)	Shape parameter $m_{PMMA800}$	Scale parameter $t_{0PMMA800}$ (s)
Gecko G1				
1 set	1.209	1617.7	\	\
Gecko G2				
1 set	1.166	885.8	\	\
2 set	\	\	1.111	108.4
Average value	1.188	1251.7	1.111	108.4

## 4. CONCLUSIONS

In this paper we have demonstrated that living geckos display adhesion times following Weibull Statistics, by performing three-dimensional surface topography characterizations and time of adhesion measurements. The Weibull shape (*i.e.*, modulus) and scale parameters can be used to describe quantitatively the statistics of the adhesion times of different geckos (male or female), materials (glass or PMMA), and interfaces (virgin or machined PMMA surfaces).

## ACKNOWLEDGMENTS

The authors would like to thank M. Biasotto of the Department of Special Surgery of the University of Trieste for experimental instruments of surface measurements, and F. Antonioli of the Department of Biomedicine, Unit of Dental Sciences and Biomaterials of the University of Trieste, for the helpful scientific discussion and surface analysis of gecko's toes. The authors are grateful to M. Buono and S. Toscano, DVM and SIVAE member, for the fundamental support for experimental studies. We gratefully acknowledge the "2I3T Scarl – Incubatore dell'Università di Torino" for SEM imaging instruments and M. G. Faga, CNR-ISTEC member, Chemical Department IFM and NIS Centre of Excellence, University of Torino for the fundamental help in performing the SEM micrographs. NMP is supported by the "Bando Ricerca Scientifica Piemonte 2006" – BIADS: Novel biomaterials for intraoperative adjustable devices for fine tuning of prostheses shape and performance in surgery.

## REFERENCES

- [1] Aristotle, *Historia Animalium*, 343 B.C. See Book IX, Part 9, translated by Thompson DAW, [http://classics.mit.edu/Aristotle/history\\_anim.html](http://classics.mit.edu/Aristotle/history_anim.html).
- [2] Simmermacher, G., *Zeitschr. Wiss. Zool.* **40**, 481–556 (1884).
- [3] Schmidt, H. R., *Jena. Z. Naturwiss* **39**, 551–580 (1904).
- [4] Dellit, W. D., *Jena. Z. Naturwiss* **68**, 613–658 (1934).
- [5] Ruiba, R. and Ernst, V., *J. Morph.* **117**, 271–294 (1965).
- [6] Autumn, K., Properties, principles and parameters of the gecko adhesive system, in *Biological Adhesives*, A. Smith and J. Callow (Eds.) (Springer Verlag, Berlin and Heidelberg, 2006), pp. 225–255; Autumn, K., "Gecko adhesion: structure, function and applications", *MRS. Bulletin* **32**, 473–478 (2007).
- [7] Russell, A. P., *J. Zool. Lond.* **176**, 437–476 (1975).
- [8] Russell, A. P., *Can J. Zool.* **64**, 948–955 (1986).
- [9] Schleich, H. H. and Kästle, W., *Amphib. Reptil.* **7**, 141–166 (1986).
- [10] Gennaro, J. G. J., *Nat. Hist.* **78**, 36–43 (1969).
- [11] Hiller, U., *Z. Morphol Tiere* **62**, 307–362 (1968).

- [12] Autumn, K. and Peattie, A., *Int. Comp. Bio.* **42**, 1081–1090 (2002).
- [13] Autumn, K., *MRS Bulletin* **32**, 473–478 (2007).
- [14] Autumn, K. and Gravish, N., *Philosophical Transactions of the Royal Society of London, Series A: Mathematical, Physical, and Engineering Sciences* **366**, 1575–1590 (2008).
- [15] Arzt, E., Gorb, S., and Spolenak, R., *Proc. Natl. Acad. Sci. USA* **100**, 10603–10606 (2003).
- [16] Autumn, K. and Peattie, A. M., *Integr. Comp. Biol.* **42**, 1081–1090 (2002).
- [17] Bergmann, P. J. and Irschick, D. J., *J. Exp. Zool.* **303A**, 785–791 (2005).
- [18] Huber, G., Gorb, S. N., Spolenak, R., and Arzt, E., *Biol. Lett.* **1**, 2–4 (2005).
- [19] Autumn, K., Dittmore, A., Santos, D., Spenko, M., and Cutkosky, M., *J. Exp. Biol.* **209**, 3569–3579 (2006).
- [20] Autumn, K., Hsieh, S. T., Dudek, D. M., Chen, J., Chitaphan, C., and Full, R. J., *J. Exp. Biol.* **209**, 260–272, 2007.
- [21] Autumn, K., Liang, Y. A., Hsieh, S. T., Zesch, W., Chan, W. P., Kenny, T. W., Fearing, R., and Full, R. J., *Nature* **405**, 681–685 (2000).
- [22] Huber, G., Mantz, H., Spolenak, R., Mecke, K., Jacobs, K., Gorb, S. N., and Arzt, E., *Proc. Natl. Acad. Sci. USA* **102**, 16293–16296 (2005).
- [23] Stork, N. E., *J. Exp. Biol.* **88**, 91–107 (1980).
- [24] Dai, Z., Gorb, S. N., and Schwarz, U., *J. Exp. Biol.* **205**, 2479–2488 (2002).
- [25] Yurdumakan, B., Raravikar, N. R., Ajayanm P. M., and Dhinojwala, A., *Chem. Commun.* **30**, 3799–3801 (2005).
- [26] Haeshin, L., Bruce, P. L., and Phillip, B. M., *Nature* **448**, 338–341 (2007).
- [27] Pugno, N. M., *J. Phys.: Condens. Matter* **19**, 395001 (17pp) (2007).